Online July 14, 2022
Journal of Neuroendovascular Therapy 2022; 16: 491–497 DOI: 10.5797/jnet.oa.2022-0024

Original Article

Evaluation of Peak Skin Doses and Lens Doses during Interventional Neuroradiology Using a Direct Measurement System

Satoru Kawauchi,[1,2,3] Koichi Chida,[2] Takashi Moritake,[4] Yusuke Hamada,[1] Shogo Yoda,[1] Hideyuki Sakuma,[1] Wataro Tsuruta,[5] and Yuji Matsumaru[6]

Objective: In interventional neuroradiology (INR), the evaluation of the peak skin dose (PSD) and lens dose is important because the patient radiation dose increases in cases in which the procedure is more difficult and complex. This study evaluated the radiation doses during INR procedures using a direct measurement system.

Methods: Radiation dose measurements during INR were performed in 332 patients with unruptured aneurysm (URAN), dural arteriovenous fistula (DAVF), and arteriovenous malformation (AVM). The PSD and bilateral lens doses were analyzed for each disease. The Pearson correlation test was used to determine whether the PSD and lens doses were linearly related to the reference air kerma ($K_{a,r}$).

Results: In all cases, the PSD and right and left lens doses were 2.36 ± 1.28 Gy, 114.2 ± 54.6 mGy, and 189.8 ± 160.3 mGy, respectively. The PSD and lens doses of the DAVF and AVM cases were significantly higher than those of the URAN case. The Pearson correlation test revealed statistically significant positive correlations between $K_{a,r}$ and PSD, $K_{a,r}$ and right lens dose, and $K_{a,r}$ and left lens dose.

Conclusion: The characteristics of radiation dose in INR were clarified. Owing to the concern of increased radiation doses exceeding the threshold values in DAVF and AVM cases, protection from radiation is required. Simple regression analysis revealed the possibility of precisely predicting PSD using $K_{a,r}$.

Keywords interventional neuroradiology, peak skin dose, lens dose, radiophotoluminescent glass dosimeter, reference air kerma

[1]*Department of Radiology, Toranomon Hospital, Tokyo, Japan*
[2]*Department of Radiological Technology, Tohoku University Graduate School of Medicine, Sendai, Miyagi, Japan*
[3]*Okinaka Memorial Institute for Medical Research, Tokyo, Japan*
[4]*Department of Radiation Regulatory Science Research, National Institute of Radiological Sciences, National Institute for Quantum Science and Technology, Chiba, Chiba, Japan*
[5]*Department of Endovascular Neurosurgery, Toranomon Hospital, Tokyo, Japan*
[6]*Division for Stroke Prevention and Treatment, Department of Neurosurgery, Faculty of Medicine, University of Tsukuba, Tsukuba, Ibaraki, Japan*

Received: April 13, 2022; Accepted: May 31, 2022
Corresponding author: Satoru Kawauchi. Department of Radiology, Toranomon Hospital, 2-2-2, Toranomon, Minato-ku, Tokyo 105-8470, Japan
Email: shibaken.shatle@kjd.biglobe.ne.jp

Introduction

With advances in medical devices and materials, interventional neuroradiology (INR) is increasingly used in the treatment of various vascular diseases of the head and neck and cardiovascular lesions. However, INR procedures are often complex, increasing the fluoroscopy time and radiation dose for patients.[1–8] Several radiation-induced skin injuries have been reported in cases of cerebral aneurysm, dural arteriovenous fistula (DAVF), and arteriovenous malformation (AVM).[9–12] Therefore, it is important to evaluate the entrance skin dose through a series of INR procedures. Moreover, it is essential to evaluate the lens dose for each patient during INR, as it is one of the most radiosensitive tissues in the human body.[13–17]

Direct measurement of the patient's skin dose with thermoluminescent dosimeters or radiophotoluminescent glass dosimeters (RPLDs) was performed during diagnostic

angiography and INR.[9,15,18–23] However, these studies did not estimate the peak skin dose (PSD) or the right and left lens doses in detail.

This study aimed to evaluate the radiation doses (PSD and bilateral lens doses) in INR procedures using a direct measurement system.

Materials and Methods

Study design and patients

This prospective study included consecutive 333 patients with unruptured aneurysm (URAN), DAVF, and AVM. The exclusion criteria were as follows: age less than 20 years (n = 0) and multiple INR procedures (n = 1). All participants provided informed consent, and the study protocol was approved by our institutional review board.

Angiogram technique

A biplane X-ray device (Allura Xper FD20/20; Philips Healthcare, Best, Netherlands) equipped with flat-panel detectors was used in this study. The lateral X-ray tube focal spot was located on the patient's left side, while in a supine position. Fluoroscopy was performed in the pulse mode at a rate of 12.5 pulses per second, with a filter of 0.4 mm Cu + 1.0 mm Al. A DSA series was performed at two or three frames per second with a filter of 0.1 mm Cu + 1.0 mm Al filter. The exposure parameters, such as tube voltage and tube current, were controlled by an automatic brightness control system for the fluoroscopy and DSA modes.

Dosimetry technique

The PSD and the right and left lens doses of the patients were measured using small RPLD chips GD-302M (Chiyoda Technol, Tokyo, Japan) and a dosimetry cap made of thin stretchable polyester (RADIREC), as described in previous studies.[9,15,19–22] The RPLD chips were placed in 64 pockets sewn into a standard dosimetry cap, as shown in **Fig. 1**. The dosimetry technique and the method used for calculating the skin doses have been described in detail in previous studies.[15,19,20] We assumed that the maximum value of all skin doses at the 64 dose-monitoring points was the PSD, and the radiation dose measured immediately above the eyeball was representative of the lens dose.

Data collection

Medical charts were retrospectively reviewed to collect patients' demographic information and procedural details. The total fluoroscopy time (TFT) and reference air kerma ($K_{a,r}$), which refer to the cumulative dose to the patient and kerma area product (P_{KA}), were obtained from the report provided by the angiography machine.

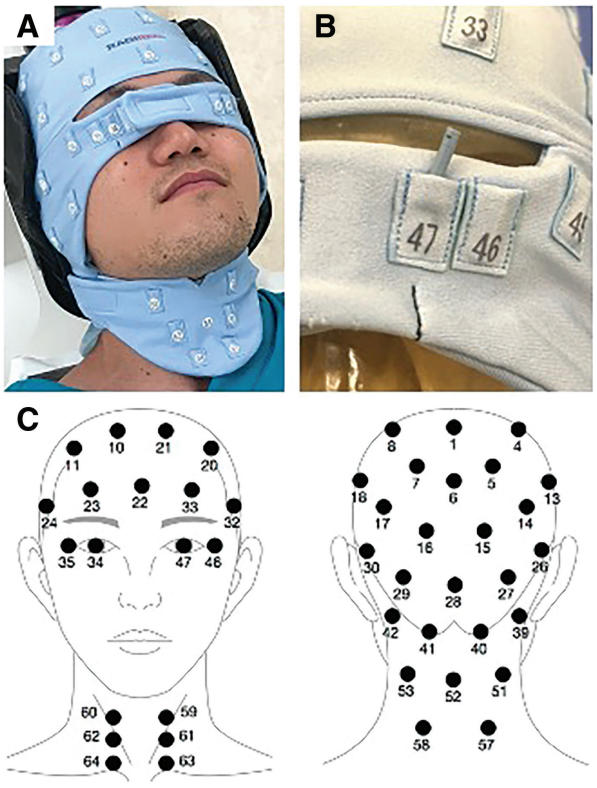

Fig. 1 Dose-monitoring system (RADIREC) in INR. (**A**) The patients wore a dosimetry cap throughout the procedure so that skin doses could be measured. (**B**) Each RPLD chip was placed into the pockets of a stretchable cap. (**C**) Dose-monitoring points for patients. PSD was defined as the maximum value of all skin doses in the 64 dose-monitoring points. Lens doses were defined as the radiation dose measured just above the eyeball. INR: interventional neuroradiology; PSD: peak skin dose; RPLD: radiophotoluminescent glass dosimeter

Statistical analysis

The right and left lens doses in the 332 cases were compared using paired t-tests. The TFT, $K_{a,r}$, P_{KA}, PSD, and bilateral lens doses for each disease were compared using the Kruskal–Wallis test. Multiple comparisons were performed between each disease group using the Dunn's test. The Pearson correlation test was used to determine whether the PSD and lens doses were linearly related to $K_{a,r}$.

Statistical analyses were performed using JMP Pro version 15.0.0 (JMP, Cary, NC, USA). A p-value of <0.05 was considered statistically significant.

Results

Table 1 summarizes the patient and angiographic characteristics (TFT, $K_{a,r}$, P_{KA}, PSD, and the right and left

Table 1 Patient demographics, angiographic parameters and radiation doses of each case

	All cases	URAN cases	DAVF cases	AVM cases
Number of cases	332	272	41	19
Age (years)	59.8 ± 12.7	60.5 ± 11.4	63.5 ± 13.1	40.6 ± 13.9
Man:woman	95: 237	66: 206	23: 18	6: 13
Body mass index	22.8 ± 3.4	22.6 ± 3.3	24.3 ± 3.2	21.7 ± 3.3
Total fluoroscopic time (min)	53.0 ± 29.9 (range: 13.0–189.3)	46.4 ± 20.7 (range: 13.0–132.0)	87.2 ± 46.5 (range: 13.4–181.8)	74.0 ± 36.7 (range: 22.1–189.3)
Reference air kerma (Gy)	4.59 ± 2.64 (range: 1.35–19.6)	3.95 ± 1.91 (range: 1.35–14.4)	6.89 ± 3.34 (range: 2.17–13.9)	8.75 ± 3.52 (range: 4.24–19.6)
Kerma area product ($Gy \cdot cm^2$)	454.5 ± 289.6 (range: 52.2–2562.8)	362.6 ± 146.7 (range: 52.2–987.1)	809.3 ± 360.3 (range: 394.3–1983.9)	991.1 ± 459.5 (range: 482.4–2562.8)
Peak skin dose (Gy)	2.36 ± 1.28 (range: 0.30–8.56)	2.02 ± 0.90 (range: 0.30–5.77)	3.45 ± 1.50 (range: 1.49–6.90)	4.60 ± 1.55 (range: 2.14–8.56)
Right lens dose (mGy)	114.2 ± 54.6 (range: 45.6–346.5)	102.3 ± 44.9 (range: 45.6–326.9)	173.4 ± 63.8 (range: 50.1–346.5)	151.5 ± 56.7 (range: 79.4–297.2)
Left lens dose (mGy)	189.8 ± 160.3 (range: 48.9–1092.6)	164.8 ± 139.2 (range: 48.9–1092.6)	313.4 ± 221.4 (range: 66.5–993.9)	268.6 ± 112.6 (range: 120.5–524.2)

All values are represented as mean ± SD. AVM: arteriovenous malformation; DAVF: dural arteriovenous fistula; SD: standard deviation; URAN: unruptured aneurysm

Table 2 Number of cases exceeding the threshold dose of the tissue reaction

	All cases (n = 332)	URAN cases (n = 272)	DAVF cases (n = 41)	AVM cases (n = 19)
PSD >2.0 Gy (%)	163 (49.1%)	110 (40.4%)	34 (82.9%)	19 (100%)
PSD >3.0 Gy (%)	73 (22.0%)	36 (13.2%)	21 (51.2%)	16 (84.2%)
Left lens dose >500 mGy (%)	17 (5.1%)	11 (4.0%)	5 (12.2%)	1 (5.3%)

AVM: arteriovenous malformation; DAVF: dural arteriovenous fistula; PSD: peak skin dose; URAN: unruptured aneurysm

lens doses). A total of 332 patients who underwent INR at our institution were analyzed for skin dose dosimetry using the RADIREC. This study included 95 men and 237 women, with a mean age of 59.8 years. There were 272 (81.9%), 41 (12.3%), and 19 (5.7%) patients with URAN, DAVF, and AVM, respectively. In the analysis of all cases, the PSD and right and left lens doses were 2.36 ± 1.28 Gy (range: 0.30–8.56 Gy), 114.2 ± 54.6 mGy (range: 45.6–346.5 mGy), and 189.8 ± 160.3 mGy (range: 48.9–1092.6 mGy), respectively. The dose to the left lens was significantly higher than that to the right (p <0.001).

Table 2 shows the number of cases that exceeded the threshold doses for early transient erythema (2.0 Gy) and temporary epilation (3.0 Gy) of the skin and cataracts in the eyes (500 mGy). The PSDs of 163 (49.1%) and 73 (22.0%) patients were >2.0 Gy and >3.0 Gy, respectively. The left lens dose was >500 mGy in 17 (5.1 %) patients.

In the analysis of each disease, TFT, $K_{a,r}$, and P_{KA} of DAVF and AVM cases were higher than those of URAN cases (p <0.001). **Figure 2** shows the PSDs and lens doses of the URAN, DAVF, and AVM cases. The mean PSDs of the URAN, DAVF, and AVM cases were 2.02 ± 0.90 Gy, 3.45 ± 1.50 Gy, and 4.60 ± 1.55 Gy, respectively. The PSDs of the DAVF and AVM cases were significantly higher than those of the URAN cases (p <0.001). The mean right lens doses of the URAN, DAVF, and AVM cases were 102.3 ± 44.9 mGy, 173.4 ± 63.8 mGy, and 151.5 ± 56.7 mGy, respectively. The right lens dose in the AVM group was significantly higher than that in the URAN group (p <0.01). The mean left lens doses of the URAN, DAVF, and AVM cases were 164.8 ± 139.2 mGy, 313.4 ± 221.4 mGy, and 268.6 ± 112.6 mGy, respectively. The left lens doses of DAVF and AVM were significantly higher than those of URAN (p <0.001). In the URAN cases, the PSDs of 110 patients (40.4%) exceeded 2.0 Gy and the PSDs were >3.0 Gy in 36 patients (13.2%). The left lens doses were >500 mGy in 11 (4.0 %) patients. In the DAVF cases, the PSDs of 34 patients (82.9%) exceeded 2.0 Gy and the PSDs were >3.0 Gy in 21 patients (51.2%). The left lens doses of five patients (12.2%) were >500 mGy. In the AVM cases, the PSDs of 19 patients (100%) exceeded 2.0 Gy and the PSDs were >3.0 Gy in 16 patients (84.2%). The left lens dose in one patient (5.3%) was >500 mGy. Among all the diseases, there were no cases in which the right lens dose exceeded 500 mGy.

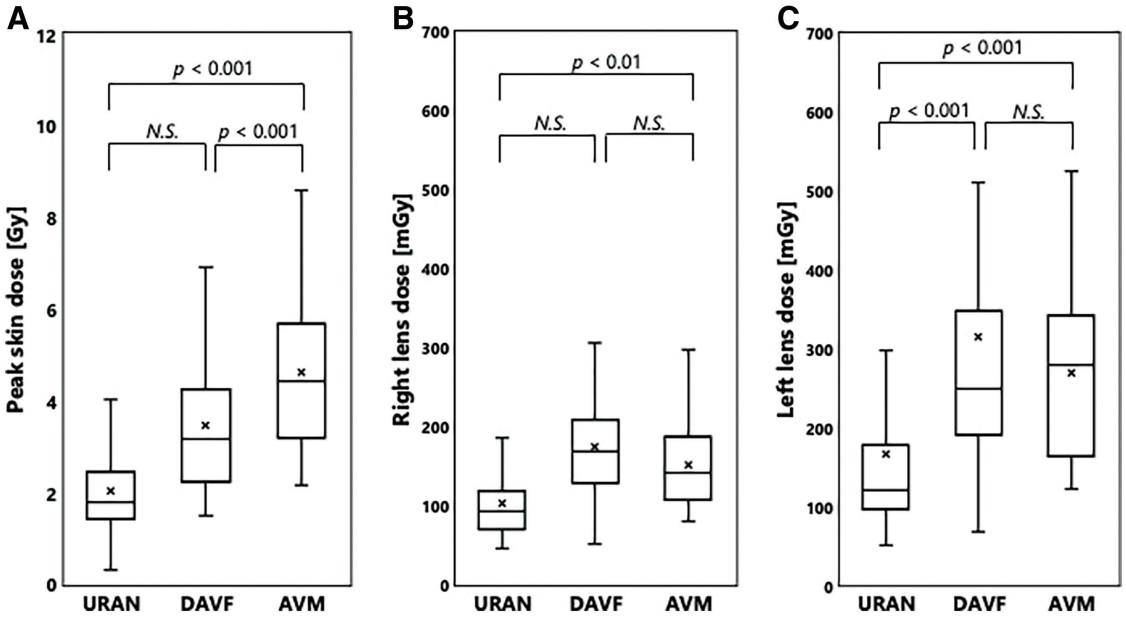

Fig. 2 Box plot of the radiation dose in INR. (**A**) PSD. (**B**) Right lens dose. (**C**) Left lens dose. AVM: arteriovenous malformation; DAVF: dural arteriovenous fistula; INR: interventional neuroradiology; N.S.: not significant; PSD: peak skin dose; URAN: unruptured aneurysm

The Pearson correlation test revealed statistically significant correlations between $K_{a,r}$ and PSD (r = 0.9737, p <0.001), $K_{a,r}$ and right lens dose (r = 0.9142, p <0.001), and $K_{a,r}$ and left lens dose (r = 0.7702, p <0.001). The regression lines drawn using the PSD, right lens dose, and left lens dose as an outcome value (y) and $K_{a,r}$ (mGy) as a predictor variable (x) can be mathematically represented as y = 0.49x (R^2 = 0.9481), y = 0.022x (R^2 = 0.8328), and y = 0.036x (R^2 = 0.5933), respectively (**Fig. 3**).

Discussion

Radiation skin injury (RSI) associated with INR, which includes early transient erythema and temporary epilation, is a well-known tissue reaction. Moreover, the International Commission on Radiological Protection published Publication 118 describing the effects of radiation on tissues and organs.[24] This report suggested that the eye lens might be more sensitive to ionizing radiation than previously thought, and a threshold for an absorbed dose of 500 mGy was suggested. Therefore, accurate evaluation of skin and lens doses is important to reduce the radiation dose.[25–27] Our direct dosimetry technique using multiple RPLDs is ideal because it can achieve precise dose distribution, including the PSD and bilateral lens doses of the patient.[21,22] Although some studies have measured the radiation dose of patients during INR using the direct dosimetry method,[28–30] no detailed analysis of the PSD and lens dose has been reported for each disease.

The mean right and left lens doses were 114.2 ± 54.6 mGy and 189.8 ± 160.3 mGy, respectively. The mean left lens dose was 1.66 times higher than that of the right lens (p <0.001) because the lateral X-ray tube was located on the left side of the patients who were placed in a supine position. These results are in good agreement with those of our previous study on flow-diverter stenting cases.[19] The lens dose closer to the X-ray tube may increase and exceed the threshold dose for cataracts. Therefore, protective measures, such as collimation of the radiation field and control of the pulse rate and frame number of the DSA, may be required.

In the analysis of the radiation dose for each disease, the PSD and lens doses of the DAVF and AVM cases were higher than those of the URAN cases. In the DAVF cases, the mean PSD was 3.45 ± 1.50 Gy and exceeded 3.0 Gy in 51.2% of the cases. The rate of left lens doses above 500 mGy was higher than that of other diseases. These results indicate that in DAVF cases, careful attention must be paid to the increased dose to the lens and skin. In the AVM cases, the mean PSD was 4.60 ± 1.55 Gy and exceeded 3.0 Gy in 84.2% of the cases. Regarding the left lens dose, only one case exceeded 500 mGy. In AVM cases, attention to the lens dose is also necessary because fluoroscopy and procedure times are extended; however, monitoring the

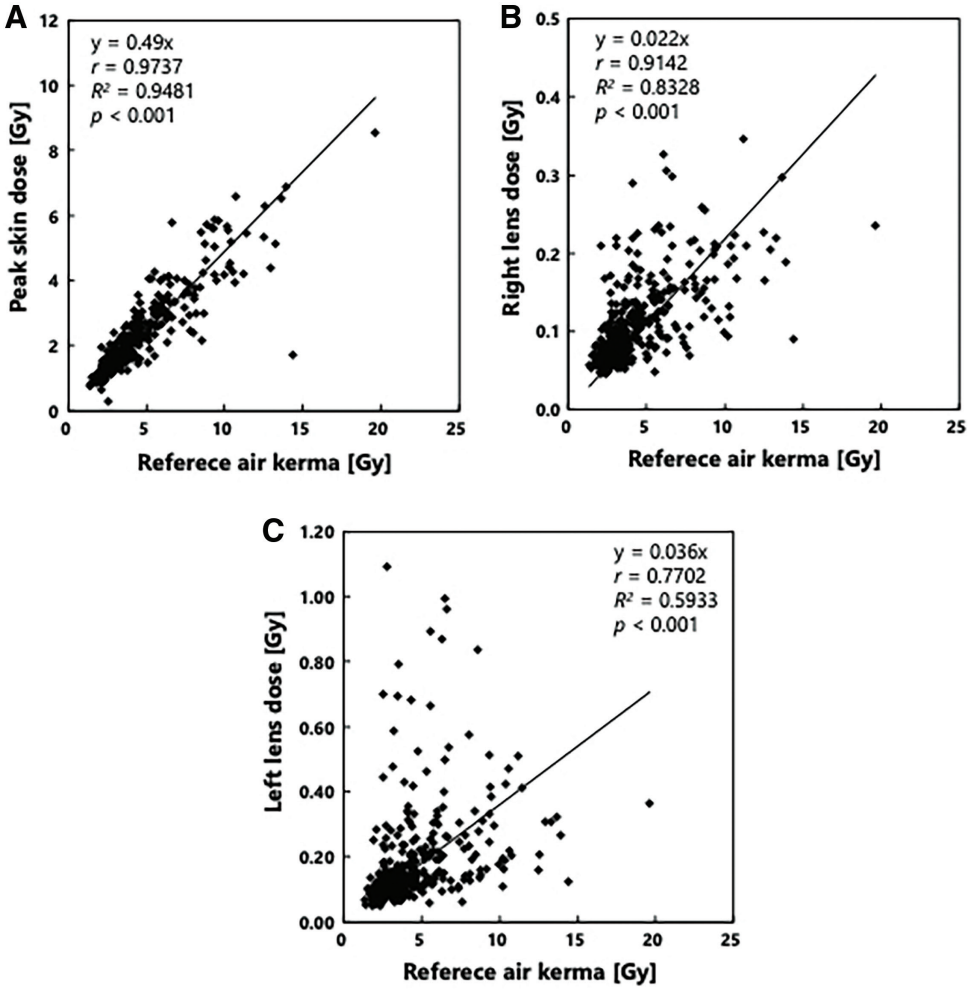

Fig. 3 Correlations between the reference air kerma and radiation dose of the patients. The lines on the graphs indicate linear regressions. (**A**) Correlation between the reference air kerma and the PSD. (**B**) Correlation between the reference air kerma and the right lens dose. (**C**) Correlation between the reference air kerma and the left lens dose. PSD: peak skin dose

skin dose is more important. Our findings showed that attention should be given to tissues due to radiation variations between diseases.

The Pearson correlation test revealed statistically significant positive correlations between the PSD and $K_{a,r}$ ($r = 0.9737$), and a simple regression analysis revealed the possibility of precisely predicting the PSD using $K_{a,r}$ ($R^2 = 0.9481$). This result is similar to that of previous reports.[19–22] PSD can be estimated accurately using $K_{a,r}$, although the prediction formula differs depending on the facility or angiographic machine. By using the PSD prediction formula, it is possible to evaluate PSD in real time, which is useful for avoiding RSI and cataracts in the INR. As with PSD, it is possible to predict the right lens dose with a high accuracy using $K_{a,r}$ ($R^2 = 0.8328$). The accuracy of the regression equation for the left lens dose was lower than that of the PSD and right lens dose ($R^2 = 0.5933$). This result was probably due to the working angle of the X-ray tubes in the INR. Although a few direct X-rays normally enter the left lens, they enter the lens depending on the setting of working angle. For INR, the dose on the left side was higher and more important. For an accurate assessment, it is desirable to measure the lens dose, as in the method used in this study.

Currently, the diagnostic reference level of angiography is being formulated in each country, most of which uses $K_{a,r}$ and P_{KA}. The diagnostic reference level is used to minimize stochastic effects and optimize the appropriate use of medical radiation. The evaluation of PSD and lens doses is important to avoid tissue reactions to the skin and lenses during high-dose exposure in INR. Thus, the $K_{a,r}$, P_{KA}, and PSD lens doses are complementary. By adding the

measured values of the PSD and lens doses or the estimated values using regression equations to the conventional dose management system using only $K_{a,r}$ and P_{KA}, it is possible to optimize radiation protection using parameters that consider biological effects.

Conclusion

In this study, patient radiation doses for URAN, DAVF, and AVM were measured using a direct measurement system. The PSD and lens doses of the DAVF and AVM cases were significantly higher than those of the URAN cases. Some DAVF cases exceeded the threshold dose for the skin and lens. PSD exceeded the threshold dose in most AVM cases, whereas the left lens dose exceeded the threshold dose in only one case. Therefore, care should be taken when increasing the skin and lens doses in patients with DAVF and AVM. The Pearson correlation test revealed statistically significant positive correlations between $K_{a,r}$ and PSD, $K_{a,r}$ and right lens dose, and $K_{a,r}$ and left lens dose. Simple regression analysis revealed the possibility of precisely predicting the PSD using $K_{a,r}$.

Funding

This study was supported by JSPS KAKENHI (grant number: JP19K17183).

Disclosure Statement

The authors declare that they have no conflicts of interest.

References

1) Chida K, Kaga Y, Haga Y, et al. Occupational dose in interventional radiology procedures. *AJR Am J Roentgenol* 2013; 200: 138–141.
2) Chida K, Kato M, Inaba Y, et al. Real-time patient radiation dosimeter for use in interventional radiology. *Phys Med* 2016; 32: 1475–1478.
3) Chida K, Ohno T, Kakizaki S, et al. Radiation dose to the pediatric cardiac catheterization and intervention patient. *AJR Am J Roentgenol* 2010; 195: 1175–1179.
4) Chida K, Saito H, Otani H, et al. Relationship between fluoroscopic time, dose-area product, body weight, and maximum radiation skin dose in cardiac interventional procedures. *AJR Am J Roentgenol* 2006; 186: 774–778.
5) Chida K, Takahashi T, Ito D, et al. Clarifying and visualizing sources of staff-received scattered radiation in interventional procedures. *AJR Am J Roentgenol* 2011; 197: W900–W903.
6) Endo M, Haga Y, Sota M, et al. Evaluation of novel X-ray protective eyewear in reducing the eye dose to interventional radiology physicians. *J Radiat Res (Tokyo)* 2021; 62: 414–419.
7) Ishii H, Chida K, Satsurai K, et al. A phantom study to determine the optimal placement of eye dosimeters on interventional cardiology staff. *Radiat Prot Dosimetry* 2019; 185: 409–413.
8) Morishima Y, Chida K, Meguro T. Effectiveness of additional lead shielding to protect staff from scattering radiation during endoscopic retrograde cholangiopancreatography procedures. *J Radiat Res (Tokyo)* 2018; 59: 225–232.
9) Hayakawa M, Moritake T, Kataoka F, et al. Direct measurement of patient's entrance skin dose during neurointerventional procedure to avoid further radiation-induced skin injuries. *Clin Neurol Neurosurg* 2010; 112: 530–536.
10) Nannapaneni R, Behari S, Mendelow D, et al. Temporary alopecia after subarachnoid haemorrhage. *J Clin Neurosci* 2007; 14: 157–161.
11) Thorat JD, Hwang PY. Peculiar geometric alopecia and trigeminal nerve dysfunction in a patient after Guglielmi detachable coil embolization of a ruptured aneurysm. *J Stroke Cerebrovasc Dis* 2007; 16: 40–42.
12) Wen CS, Lin SM, Chen Y, et al. Radiation-induced temporary alopecia after embolization of cerebral arteriovenous malformations. *Clin Neurol Neurosurg* 2003; 105: 215–217.
13) Kawauchi S, Chida K, Hamada Y, et al. Lens dose reduction with a bismuth shield in neuro cone-beam computed tomography: an investigation on optimum shield device placement conditions. *Radiol Phys Technol* 2022; 15: 25–36.
14) Kawauchi S, Chida K, Moritake T, et al. Radioprotection of eye lens using protective material in neuro cone-beam computed tomography: estimation of dose reduction rate and image quality. *Phys Med* 2021; 82: 192–199.
15) Kawauchi S, Chida K, Moritake T, et al. Estimation of patient lens dose associated with C-arm cone-beam computed tomography usage during interventional neuroradiology. *Radiat Prot Dosimetry* 2019; 184: 138–147.
16) Matsunaga Y, Chida K, Kondo Y, et al. Diagnostic reference levels and achievable doses for common computed tomography examinations: results from the Japanese nationwide dose survey. *Br J Radiol* 2019; 92: 20180290.
17) Sakamoto H, Moritake T, Sun L, et al. Monitoring and protection against radiation dose to eyes of operators performing neuroendovascular procedures: a nationwide study in Japan. *JNET J Neuroendovasc Ther* 2022; 16: 354–360.

18) Kato M, Chida K, Moritake T, et al. Direct dose measurement on patient during percutaneous coronary intervention procedures using radiophotoluminescence glass dosimeters. *Radiat Prot Dosimetry* 2017; 175: 31–37.
19) Kawauchi S, Chida K, Moritake T, et al. Treatment of internal carotid aneurysms using pipeline embolization devices: measuring the radiation dose of the patient and determining the factors affecting it. *Radiat Prot Dosimetry* 2020; 188: 389–396.
20) Kawauchi S, Moritake T, Hayakawa M, et al. Estimation of maximum entrance skin dose during cerebral angiography. *Jpn J Radiol Technol* 2015; 71: 746–757. (in Japanese)
21) Moritake T, Hayakawa M, Matsumaru Y, et al. Precise mapping system of entrance skin dose during endovascular embolization for cerebral aneurysm. *Radiat Meas* 2011; 46: 2103–2106.
22) Moritake T, Matsumaru Y, Takigawa T, et al. Dose measurement on both patients and operators during neurointerventional procedures using photoluminescence glass dosimeters. *AJNR Am J Neuroradiol* 2008; 29: 1910–1917.
23) Sun L, Mizuno Y, Iwamoto M, et al. Direct measurement of a patient's entrance skin dose during pediatric cardiac catheterization. *J Radiat Res (Tokyo)* 2014; 55: 1122–1130.
24) The 2007 recommendations of the International Commission on Radiological Protection. ICRP publication 103 *Ann ICRP* 2007; 37: 1–332.
25) Haga Y, Chida K, Kaga Y, et al. Occupational eye dose in interventional cardiology procedures. *Sci Rep* 2017; 7: 569.
26) Kato M, Chida K, Ishida T, et al. Occupational radiation exposure dose of the eye in department of cardiac arrhythmia physician. *Radiat Prot Dosimetry* 2019; 187: 361–368.
27) Kato M, Chida K, Ishida T, et al. Occupational radiation exposure of the eye in neurovascular interventional physician. *Radiat Prot Dosimetry* 2019; 185: 151–156.
28) Sánchez RM, Vano E, Fernandez JM, et al. Radiation doses in patient eye lenses during interventional neuroradiology procedures. *AJNR Am J Neuroradiol* 2016; 37: 402–407.
29) Sandborg M, Rossitti S, Pettersson H. Local skin and eye lens equivalent doses in interventional neuroradiology. *Eur Radiol* 2010; 20: 725–733.
30) Suzuki S, Furui S, Matsumaru Y, et al. Patient skin dose during neuroembolization by multiple-point measurement using a radiosensitive indicator. *AJNR Am J Neuroradiol* 2008; 29: 1076–1081.